

Photoluminescence emission through thin metal films via coupled surface plasmon–polaritons

S. WEDGE*[†], S. H. GARRETT[†], I. SAGE[‡] and W. L. BARNES[†]

[†]Thin Films Photonics Group, School of Physics, University of Exeter,
Stocker Road, Exeter, EX4 4QL, UK

[‡]Photonics and Displays Group, QinetiQ, St Andrews Road, Malvern,
Worcestershire WR14 3PS, UK

(Received 15 July 2004)

We present experimental results showing the variation in photoluminescence from an organic material emitted through a thin metal film as successive dielectric overlayers are added to the far side of the metal. The intensity of the emission from the structure is examined as the surface plasmon–polariton (SPP) modes associated with the two metal surfaces evolve with increasing overlayer thickness from individual to coupled SPP modes. The SPP modes are scattered to produce light by the addition to the metal film of wavelength-scale periodic microstructure. We show that the addition of a dielectric overlayer of an appropriate thickness to the metal film is accompanied by an increase in the intensity of the emission by a factor of 3 over a similar structure with no dielectric overlayer, and by a factor of 50 over a similar planar structure. We show that this increase in emission is mediated via coupled SPP modes.

1. Introduction

The emission of light through a metal film continues to attract attention, both to explore the underlying physics further, and because such studies are of relevance to light-emitting devices. In particular, the development of commercially available organic light-emitting diodes (OLEDs) places continuing demands to find ways to increase the efficiency of these devices. The internal efficiency of OLEDs has approached unit efficiency so that improvements to the optical out-coupling efficiency of these structures are becoming increasingly important. The standard configuration of an OLED consists of an organic emissive material bounded on one side by a thick metallic cathode and on the other by a transparent anode and glass substrate, with emission taking place through the anode and substrate. Recently it has been demonstrated that a top-emitting OLED may be produced on an opaque substrate, emission taking place through a thin metal cathode [1–3]. The ability to integrate such a device on to an opaque substrate such as silicon provides potential for display applications. For such devices the optical out-coupling must take place through the metallic cathode, and it is some of the implications that this has for the optical efficiency of these structures that we address here.

*Corresponding author. Email: S.Wedge@exeter.ac.uk

One important aspect in exploring out-coupling from OLEDs are the surface plasmon–polariton (SPP) modes associated with the surfaces of the metallic cathode. SPPs are trapped surface modes that have electromagnetic fields that decay exponentially into both the surrounding metal and the dielectric media; on a planar surface they are non-radiative in nature. Previous work [4, 5] has shown that such SPP modes can act to quench the emission from the organic material and thus to detract from device efficiency, in some cases trapping more than 30% of the light emitted in substrate-emitting OLEDs. In a top-emitting device where the cathode is bound on either side by different dielectrics, for example air on one side and an organic emissive material on the other, the cathode may support two distinct SPP modes, one associated with each metal–dielectric interface. Emission that takes place into these modes detracts from device efficiency so that methods of recovering this energy are being explored as a means to improve device efficiency [6].

As we have recently shown, the SPP mode associated with the metal–organic interface dominates the power lost by emitters to SPP modes in top-emitting structures [7]. To increase the out-coupling efficiency the power lost to this mode needs to be recovered, something that can be done by Bragg scattering from periodic microstructure [8–10]. However, for power lost to the SPP mode associated with the metal–organic interface to be recovered, not only must it be scattered so as to produce light, but also it must cross the metal film. Emission mediated via the SPP mode associated with the metal–organic interface may take place through the metal by one of two routes. Firstly, the SPP may scatter from the metal–organic interface; in then crossing the metal film, however, the resulting emission will be diminished by attenuation in the metal. Alternatively, the fields associated with the metal–organic SPP that extend across the metal may be scattered to light from the microstructure at the metal–air interface. Whilst emission mediated via this route may take place directly into the air, the field associated with the metal–organic interface SPP decays exponentially across the metal, again resulting in a loss of energy and a reduction in the potential emission. In order therefore to maximize emission via the recovery of the energy lost to the SPP mode associated with the metal–organic interface a means must be sought to allow the fields associated with this SPP to span the metal. There are two ways in which this may be done. The first is to match the wave vectors of the SPP modes at the two metal–dielectric interface. Such an approach has been utilized by SPP cross-coupling, where wavelength-scale periodic microstructure in the form of a grating (pitch λ_g) is introduced into the metal so as to allow Bragg scattering of the SPP modes [11]. The grating pitch is chosen so that the wave vector of the SPP at the metal–organic boundary may be matched to the SPP mode at the metal–air interface when the following grating coupling condition is met:

$$\pm \mathbf{k}_{\text{SPPair}} = \pm \mathbf{k}_{\text{SPPorg}} \pm n \mathbf{k}_g, \quad (1)$$

where $\mathbf{k}_{\text{SPPair}}$ and $\mathbf{k}_{\text{SPPorg}}$ are the wave vectors of the SPP modes associated with the metal–air and the metal–organic interfaces respectively, \mathbf{k}_g is the grating vector (equal to $2\pi/\lambda_g$) and n is the order of the scattering process. The SPP at the metal–air interface may then in turn couple to radiation, again via the grating

$$\pm \mathbf{k}_{\text{SPPair}} = \pm \mathbf{k}_0 \sin \theta \pm n \mathbf{k}_g, \quad (2)$$

where \mathbf{k}_0 is the free-space wave vector and θ the emission angle of the emitted light. This cross-coupling technique has been reported as a means of transporting molecular fluorescence across a thin metal film [12]. However, as emission mediated via cross-coupled SPP modes is dependent upon two coupling conditions (equations (1) and (2)), the resulting emission occurs only over a very narrow range of emission angles and wavelengths [11]. Owing to the high directionality and narrow wavelength spread of this emission such an approach is far from ideal for applications such as displays.

A second and alternative means of transporting energy across a thin metal film may be sought by employing a metal film that is bound on each side by matched dielectric media. For a thick metal film, such a structure supports only one SPP mode. However, if the metal film thickness is such that the fields associated with each metal dielectric interface can overlap, then the structure may support a pair of degenerate coupled SPP modes [13]. One mode has a symmetric charge distribution at the metal–dielectric interface with respect to the midpoint of the metal, the other has an asymmetric charge distribution. These different charge distributions, together with their associated field distributions, lift the degeneracy of the coupled SPP modes, the mode with the symmetric charge distribution having a higher energy (frequency) than the SPP with the asymmetric charge distribution for a given wave vector.

In a structure containing a thin metal film, coupled SPP modes have fields that may span the metal, thus providing a way for energy to cross the metal [14]. However, to recover the energy lost to the SPP modes they must be coupled to light in the far field. Again, out-coupling of the SPP modes may be achieved by incorporating into the metal film a wavelength-scale periodic microstructure, thus allowing the SPPs to Bragg scatter the light. Such a scheme, in which a thin corrugated metal film is bound on either side by dielectric media whose effective refractive indices are matched, has already been used to demonstrate that the energy lost to the SPP mode associated with the metal–organic interface may be transported across the metal film and then coupled to light in the far field [14]; here we investigate the process in more detail.

The previous study by Gruhlke *et al.* [14] presented data showing the intensity of angle-dependent photoluminescence (PL) emission through a thin metal film in the near infrared (850 nm). Here, we show the intensity of angle-dependent PL mediated via coupled SPPs across the visible spectrum (416–806 nm). We also present PL emission data from a structure that supports two individual SPP modes, one associated with each interface of the metal film as successive thin dielectric overlayers are added to the metal–air interface. The addition of these dielectric overlayers on to the metal increases the effective refractive index at the metal–air boundary. When the indices of the two dielectric media bounding the metal are matched, the degenerate SPP modes supported by the system may interact and couple together. Such an approach allows for a direct comparison between the intensity of the PL emission from a structure that supports individual SPP modes with the PL from a structure where the media bounding the metal are matched and therefore support a pair of coupled SPPs. By incrementally building up the thickness of the dielectric overlayer at the metal–air interface the PL intensity may be monitored as the SPPs modes change from individual to coupled modes.

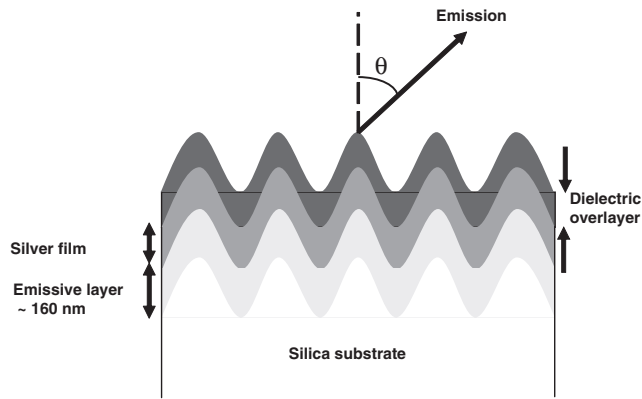


Figure 1. Schematic diagram of one of the structures used in our experiments.

2. Sample fabrication

A schematic cross-section of the one of the structures used in our experiments is shown in figure 1. To fabricate the grating profile, silica substrates were spin coated with a photoresist film (Shipley Megaposit SPR 700-1.2) approximately 300 nm thick. This film was exposed to a laser interference pattern from a 325 nm He–Cd laser and chemically developed to create a 338 ± 1 nm pitch microstructure (grating depth, about 50 nm). The grating profile was transferred into the silica substrate by reactive ion etching with CHF_3 and O_2 gases. An emissive layer was added by doping a polymer, poly(methyl methacrylate) (PMMA), with the organic material, tris(8-hydroxyquinoline)aluminium (Alq_3) (3 wt%); this was applied by means of spin coating to give a film approximately 160 nm thick. The effective refractive index of the resulting emissive layer was taken to be equal to that of PMMA, about 1.51. A thin silver film 43 ± 2 nm thick was then added by means of thermal evaporation under vacuum (10^{-7} m Torr).

As previously noted, in order to couple the SPPs on either side of the metal film the effective refractive indices of the media bounding either side of the metal must be matched. We achieved this matching by building up layers of a dielectric material on top of the metal until the effective refractive indices of the two materials bordering the metal film were equal. To this end monolayers of the material 22-tricosenoic acid (22-tric) were deposited on to the metal film using the Langmuir–Blodgett (LB) technique [15]. This technique allows nanometre control of the thickness of the dielectric overlayer, and thus great control over the effective refractive index of the upper half-space. The LB technique involves spreading a monolayer of 22-tric on to the surface of ultrapure water. Each sample was then dipped at a rate of $0.25 \times 10^{-3} \text{ ms}^{-1}$, vertically through the water surface, thereby transferring a monolayer of 22-tric on to the sample surface, a second monolayer was deposited as the sample was withdrawn, thus forming a bilayer. A known number of bilayers, each with a thickness of 5.2 nm, could therefore be added to each sample by repeated dipping. By increasing the thickness of the dielectric film in this way the effective refractive index at the metal–air boundary could be varied from 1 (bare metal) to about 1.58 for a semi-infinite LB film thickness.

In our experiment the PL emitted through the Ag film was studied as the thickness of the dielectric overlayer was varied from 0 to 197.6 nm (from 0 to 38 bilayers). The emission of light could therefore be monitored as the transition from individual to coupled SPP modes was made.

3. Transmission measurements and modal analysis

Before studying the PL emission from each structure it was first useful to explore the various modes supported by the samples used in our experiment. This we achieved by measuring the transmittance through each of the structures as a function of both the angle of incidence and the wavelength of the light incident upon the sample. From these data a dispersion map was constructed by converting the collected data to transmittance as a function of both the angular frequency and the in-plane wave vector (the in-plane wave vector being the component of the wave vector in the plane of incidence and parallel to the layers of the structure). Figure 2 shows such a dispersion map for a sample with a dielectric overlayer thickness of 46.8 nm. The z axis of this plot represents intensity of the transmission, with light regions corresponding to areas of high transmission. From figure 2, a number of transmission minima may be seen; these features were seen when a polarizer set to pass transverse magnetic (TM) polarized light was placed in front of the detector and were not evident when the polariser was set to pass transverse electric (TE) polarized light. From the TM nature of these minima together with comparison with data generated by numerical modelling (not shown) we conclude that these features correspond to incident light coupling to SPP modes associated with the Ag–organic and the Ag–dielectric overlayer–air interfaces as indicated in figure 2.

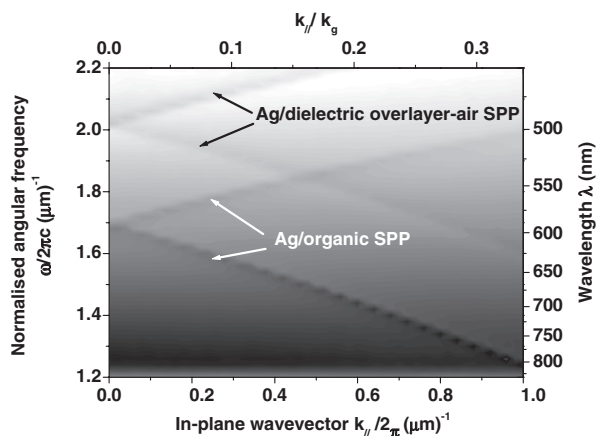


Figure 2. Dispersion map of the TM polarized transmission through a sample with a dielectric overlayer thickness of 46.8 nm. Light regions indicate areas of high transmittance. The maximum transmittance was 13%.

4. Photoluminescence measurements

To measure the PL through the Ag films, each sample was mounted on a rotation stage and the emission measured over a range of polar emission angles θ (see figure 1). The emissive layer was optically pumped through the silica substrate with a 410 nm diode laser, the resulting PL being collected through a small circular aperture that limited the angular acceptance of the emission to approximately 1° . On passing through a polarizer, set to pass either TM or TE polarized light, the collected light was focused on to an optical fibre connected to a spectrometer and a charge-coupled device detector (resolution $\Delta\lambda = 2$ nm). In order to keep the pumping conditions constant the pump angle relative to the sample was maintained constant throughout each experiment.

5. Results

We recorded PL spectra over a range of emission angles from each sample, thus allowing us to monitor any changes in the dispersion of the emission features as a function of the dielectric overlayer thickness. These spectra were converted to intensity as a function of both angular frequency and in-plane wave vector and built up to form dispersion maps. Figures 3 and 4 show dispersion maps for structures with dielectric overlayers 46.8 nm (figure 3(b)), 156.0 nm (figure 4(a)) and 197.6 nm (figure 4(b)) thick, and for a control sample (figure 3(a)) having a bare Ag film. The z axis of these plots represents emission intensity, with light regions indicating areas of strong emission. Examination of the PL data from the structure with a dielectric overlayer thickness of 46.8 nm (figure 3(b)) shows a number of PL emission maxima. Comparing this plot with the transmittance data from the same sample, shown in figure 2, it may be seen that these maxima correspond to features previously

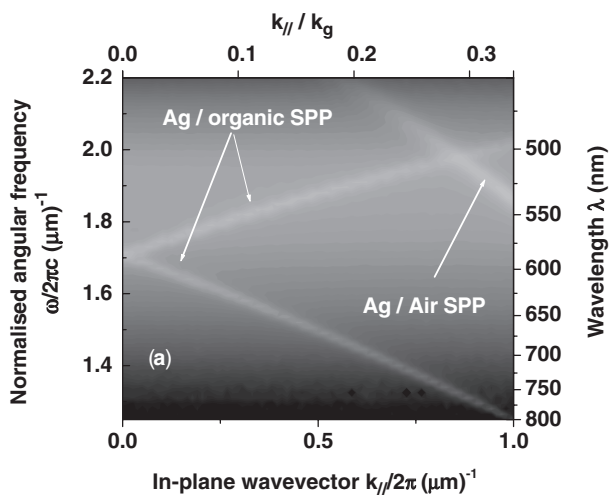


Figure 3. Dispersion maps showing the TM polarized PL emission from structures with (a) no dielectric overlayer and (b) a dielectric overlayer thickness of 46.8 nm. Light regions indicate areas of strong emission.

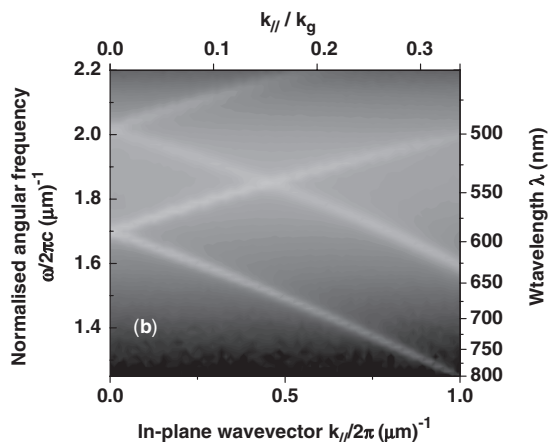


Figure 3. Continued.

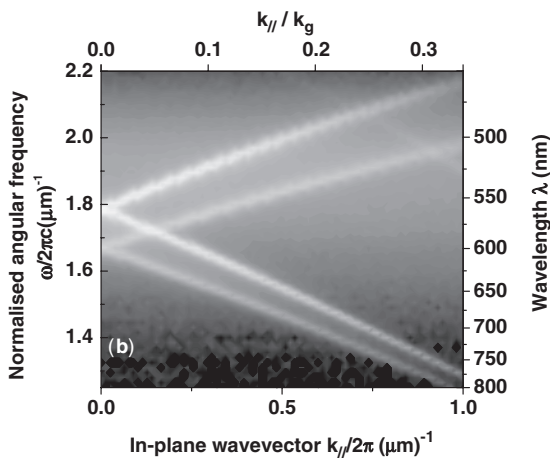
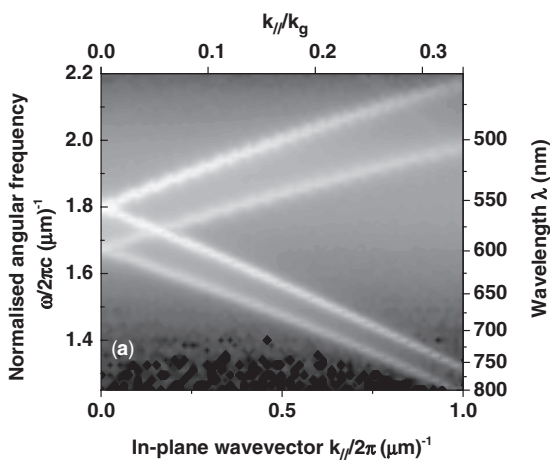


Figure 4. Dispersion maps showing the TM polarized PL emission from structures with dielectric overlayer thicknesses of (a) 156.0 nm and (b) 197.6 nm. Light regions indicate areas of strong emission.

identified as the SPP modes associated with the Ag–organic and Ag–dielectric overlayer–air interfaces.

Comparing the position of the SPP mode associated with the Ag–dielectric overlayer–air interface from the PL data for the bare metal sample (figure 3(a)) with the same mode for a sample with a dielectric thickness of 46.8 nm (figure 3(b)) it may be seen that the addition of the dielectric overlayer causes this mode to shift downwards in frequency. This downshift results from an increase in the wave vector of the SPP mode associated with the Ag–air (now Ag–dielectric overlayer–air) boundary as the effective refractive index at this interface increases with the addition of successive dielectric overlayers. This decrease in frequency continues as the dielectric film thickness is further increased to 156.0 nm (figure 4(a)). For dielectric overlayer thicknesses greater than 156.0 nm the position of the metal–dielectric overlayer–air SPP remains largely unchanged in frequency (figure 4(b)).

It might be expected that for a given in-plane wave vector the two coupled modes would have the same frequency and therefore the PL emission from a structure with a coupled geometry would only show evidence of a single mode. However, as noted above, the degeneracy of the modes is lifted when they couple and this causes the SPPs to have two different energies (frequencies). The observation of two modes at different frequencies (figure 4(a)), when the effective indices of the bounding media are matched is therefore consistent with a structure supporting coupled SPP modes and is in agreement with the findings of Gruhlke *et al.* [14].

The results discussed above indicate that, by coupling the SPP modes on either side of the metal film through matching of the effective refractive indices of the dielectric media, an increased transfer of power across the metal is possible. An important question is whether transfer of energy from the metal–organic interface to the metal–(dielectric–) air boundary is accompanied by an increase in the PL emission from the structure. To ascertain whether this was the case the intensity of the PL emission spectra from each of the structures were compared in greater detail.

Figure 5 shows PL emission spectra from each of the structures for which measurements were given in figures 3 and 4, at a fixed polar emission angle of 5° and on a logarithmic intensity scale. Also shown is the emission spectrum from a planar control sample which was identical to the bare metal sample but without the microstructure. It may be seen from figure 5 that the peak emission intensity from each structure increases with the addition of successive dielectric overlayers until a thickness of 156.0 nm is reached. For overlayer thicknesses greater than this (e.g. 197.6 nm) the peak emission intensity may be seen to fall. In each case it should be noted that the peak emission intensity was at least 30 times greater than that from the planar control sample.

To identify whether this increased emission occurred over a range of emission angles, the integrated PL emission from each sample were compared. This was achieved by summing the spectra obtained for a range of polar angles, in 1° intervals ranging from 0 to 40° from each sample and plotting this summed intensity as a function of wavelength. The area under each of these curves over a wavelength range from 416 to 806 nm was then determined by integration to give a measure of the relative emission intensity from each structure.

Figure 6 shows this integrated emission intensity for both TM and TE polarized emission as a function of dielectric overlayer thickness. Also shown is the integrated TM polarized emission intensity from the planar control sample. It may be seen from figure 6 that for relatively thin overlayers (26.0–67.6 nm) the intensity of the TM

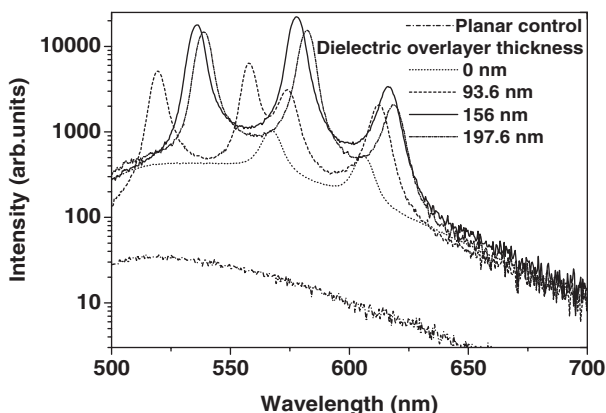


Figure 5. TM polarized PL emission intensity as a function of emission wavelength from a planar control structure and corrugated samples with dielectric overlayer thicknesses of 0, 93.6, 156.0 and 197.6 nm. Each emission spectrum was taken at an emission angle θ of 5° .

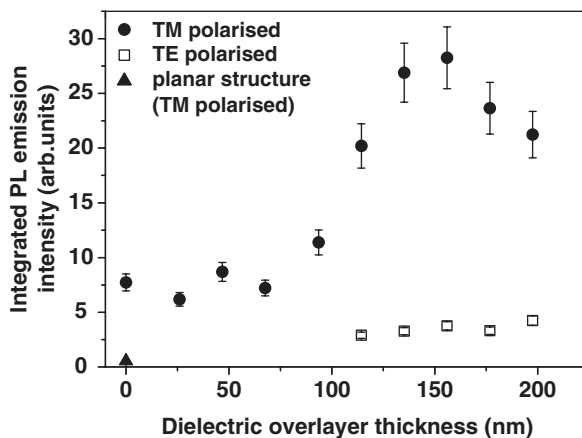


Figure 6. Integrated intensity of PL emission as a function of dielectric overlayer thickness from corrugated samples. Also shown is the integrated TM polarized PL emission intensity from a planar control structure. (Note that for dielectric overlayer thicknesses below 114.4 nm no TE polarized emission features were seen.)

polarized PL is the same as that from the sample with no overlayer, that is a bare metal film (to within experimental error). For dielectric film thicknesses greater than about 75 nm the PL emission intensity is seen to increase sharply until a maximum is reached for a dielectric thickness of 156.0 nm. For dielectric overlayer thicknesses greater than about 156.0 nm the emission intensity may be seen to fall.

The data seen in figure 6 may be understood by considering the interaction between the SPP modes associated with either side of the metal film. For the case where there is no overlayer the SPP modes associated with the two surfaces are distinct and uncoupled. As the thickness of the dielectric overlayer increases, so the effective index seen by the two modes becomes closer, eventually being matched for an overlayer thickness of 156.0 nm. As coupling takes place, energy may be transported by the coupled modes across the metal film, this transfer being optimized

when the modes are best coupled, that is for an overlayer thickness of 156.0 nm. As the thickness of the dielectric overlayer is further increased, the effective refractive indices on the two sides of the metal film gradually diverge so that coupling is reduced, thus leading to a fall in PL for higher overlayer thicknesses.

From figure 6 it may be seen that for a dielectric overlayer thickness of 156.0 nm, corresponding to an optimum coupled between the SPP modes that the integrated TM polarized PL emission is more than three times the PL from a corrugated bare metal film and 50 times the PL from the planar control structure.

In order to ensure that the fall in the emission intensity seen from structures with a dielectric overlayer of greater than 156.0 nm did not arise because power from the emitter was lost to guided modes in the dielectric film as the thickness of this film increased sufficiently to act as a waveguide, measurements were also taken of the TE polarized emission. Evidence of guided modes were not seen for dielectric film thicknesses of less than 100 nm, the intensity of the TE polarized emission from these samples being approximately equal to that seen from the planar structure. For samples with a dielectric overlayer thickness greater than 100 nm, a peak in the TE polarized emission corresponding to a guided mode was seen. These TE polarized PL emission data were summed and integrated in a manner identical with the treatment of the TM polarized data described above. From figure 6 it may be seen that there is no increase in TE polarized emission with increasing dielectric film thickness. These results indicate that the fall in the TM polarized emission intensity from the structures with a relatively thick dielectric overlayer (176.8 and 197.6 nm) is due to a decrease in the coupling of the SPP modes rather than to a redistribution of the power from the SPP modes to TE guided modes.

6. Conclusions

We have shown that the addition of a dielectric overlayer to a thin metal film may allow the transport of molecular fluorescence across the metal via coupled SPPs. These coupled SPP modes may then scatter from a wavelength-scale microstructure to produce emitted light. Data have been presented detailing the rise in PL emission intensity that occurs as the SPP modes supported by the two boundaries of the metal film evolve from individual to coupled modes as a dielectric overlayer is added. The strength of integrated PL emission from a corrugated structure that supports coupled SPPs was shown to be three times that of a similar sample with a bare corrugated metal film, and over 50 times that from a bare planar structure. This increase in emission from a structure incorporating a metal film containing a periodic microstructure topped with an appropriate dielectric overlayer may have potential in increasing the optical efficiency of devices such as top-emitting OLEDs.

Acknowledgments

This work was supported by the Materials Domain of the UK Ministry of Defence Corporate Research Program and partly funded by the UK Engineering and Physical Sciences Research Council.

References

- [1] G. Gu, V. Bulovic, P.E. Burrows, *et al.*, Appl. Phys. Lett. **68** 2606 (1996).
- [2] G. Parathasarathy, P.E. Burrows, V. Khalfin, *et al.*, Appl. Phys. Lett. **72** 2138 (1998).
- [3] L.S. Hung, C.W. Tang, M.G. Mason, *et al.*, Appl. Phys. Lett. **78** 544 (2001).
- [4] L.H. Smith, J.A.E. Wasey and W.L. Barnes, Appl. Phys. Lett. **84** 2986 (2004).
- [5] P.A. Hobson, J.A.E. Wasey, I. Sage and W.L. Barnes, IEEE J. Selected Top. Quant. Electron. **8** 378 (2002).
- [6] P.A. Hobson, S. Wedge, J.A.E. Wasey, *et al.*, Adv. Mater. **14** 1393 (2002).
- [7] S. Wedge, I.R. Hooper, I. Sage and W.L. Barnes, Phys. Rev. B **69** 245418 (2004).
- [8] J. Vuckovic, M. Loncar and A. Scherer, IEEE J. Quant. Electron. **36** 1131 (2000).
- [9] R. Windisch, S. Schoberth, S. Meinischmidt, *et al.*, J. Optics A: Pure Appl. Optics **1** 512 (1999).
- [10] W.L. Barnes, J. Lightwave. Technol. **17** 2170 (1999).
- [11] R.W. Gruhlke, W.R. Holland and D.G. Hall, Phys. Rev. Lett. **56** 2838 (1986).
- [12] D.K. Gifford and D.G. Hall, Appl. Phys. Lett. **80** 3679 (2002).
- [13] D. Sarid, Phys. Rev. Lett. **47** 1927 (1981).
- [14] R.W. Gruhlke, W.R. Holland and D.G. Hall, Optics Lett. **12** 364 (1987).
- [15] R.M. Amos and W.L. Barnes, Phys. Rev. B **55** 7249 (1997).